Polarimetric Decompositions for Soil Moisture Retrieval from Vegetated Soils in TERENO Observatories

Thomas Jagdhuber[1], Irena Hajnsek[2,1], Konstantinos P. Papathanassiou[1]

[1]Microwave and Radar Institute, German Aerospace Center (DLR), PO BOX 1116, 82234 Wessling, Germany, Phone/Fax: +49-8153-28-2329 / -1449

[2]ETH Zurich, Institute of Environmental Engineering, HIF D28.1, Schafmattstr. 6, CH-8093 Zurich

Email: Thomas.Jagdhuber@dlr.de, Irena.Hajnsek@dlr.de, Kostas.Papathanassiou@dlr.de

ABSTRACT

A refined hybrid polarimetric decomposition and inversion method for soil moisture estimation under vegetation is investigated for its potential to retrieve soil moisture from vegetated soils in TERENO observatories. The refined algorithm is applied on L-band fully polarimetric data acquired by DLR's novel F-SAR sensor. Two flight and field measurement campaigns were conducted in 2011 and 2012 for the TERENO Harz, Eifel and DEMMIN observatories, located all across Germany. The applied algorithm reveals distinct potential to invert soil moisture with inversion rates higher than >98% for a variety of crop types, phenological conditions and for pronounced topography. A quality assessment is conducted by validation with FDR, TDR and a wireless soil moisture network. The RMSE stays below 6.1vol.% for the different test sites and data takes including a variety of vegetation types in different phenological stages.

1. INTRODUCTION

The initiative for Terrestrial Environmental Observatories (TERENO) of the German Helmholtz Association tries to assess the impact of land use changes, climate changes, socioeconomic developments and human interventions in terrestrial systems by an interdisciplinary research approach on the regional scale [1].

Figure 1: Overview of the four TERENO observatories in Germany [2].

Therefore four terrestrial environmental observatories across Germany were selected to investigate the shift in environmental conditions caused by climate change (Fig. 1). These observatories are equipped with a variety of geo-physical instruments to monitor on different scales the long-term changes on eco-systems. Hence, they form an ideal test bed for analysis of soil moisture estimation with remote sensing platforms. In order to support flood forecasting or precision farming techniques the spatial assessment of soil moisture is of great benefit. Polarimetric SAR remote sensing is capable to cover these large areas. Since most of the landscape in middle latitudes is at least seasonally covered by vegetation, the estimation of soil moisture increases in complexity due to the presence and gradual increase of vegetation along the growing season. For this paper a developed hybrid polarimetric decomposition is refined for an improved soil moisture inversion under vegetation cover [3].

2. REFINED HYBRID POLARIMETRIC DECOMPOSITION FOR SOIL MOISTURE INVERSION

Soil moisture retrieval under vegetation cover involves soil and vegetation components. Therefore the recorded polarimetric SAR signature ($[T_{Data}]$) is decomposed into three canonical scattering components (surface $[T_S]$, dihedral $[T_D]$ and volume $[T_V]$) using an analytically-solvable, polarimetric hybrid decomposition algorithm [3]. In Fig. 2 the scheme for the decomposition and inversion algorithm describes the single steps within the algorithm.

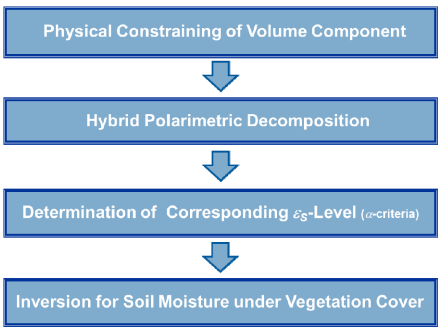

Figure 2: Scheme of hybrid polarimetric decomposition and inversion for soil moisture under vegetation cover.

$$[T_{Data}]-[T_V]=[T_G]=[T_S]+[T_D]$$

$$\begin{bmatrix} T_{11} & T_{12} & 0 \\ T_{12}^* & T_{22} & 0 \\ 0 & 0 & T_{33} \end{bmatrix} - f_v \begin{bmatrix} V_{11} & V_{12} & 0 \\ V_{12}^* & V_{22} & 0 \\ 0 & 0 & V_{33} \end{bmatrix} = \begin{bmatrix} f_s \cos\alpha_s^2 + f_d \sin\alpha_d^2 & (f_d - f_s)\cos\alpha_{d,s}\sin\alpha_{d,s} & 0 \\ (f_d - f_s)\cos\alpha_{d,s}\sin\alpha_{d,s} & f_d \cos\alpha_d^2 + f_s \sin\alpha_s^2 & 0 \\ 0 & 0 & 0 \end{bmatrix} \quad (1)$$

$$f_{d,s} = \frac{1}{2}\left(T_{11} + T_{22} - f_V V_{11} - f_V V_{22} \pm \sqrt{\left| -4\left(T_{22}\left(T_{11} - f_V V_{11}\right) + \left(T_{12} - f_V V_{12}\right)\left(f_V V_{12} - T_{12}^*\right) + f_V\left(f_V V_{11} - T_{11}\right)V_{22}\right) + \left(T_{11} + T_{22} - f_V\left(V_{11} + V_{22}\right)\right)^2 \right|} \right) \quad (2)$$

$$\alpha_{d,s} = \arccos\left(\left(1 + 4 \left| \frac{T_{12}^* - f_V V_{12}}{T_{11} - T_{22} - f_V V_{11} + f_V V_{22} \pm \sqrt{\left| T_{11}^2 + \left(T_{22} + f_V V_{11}\right)^2 + 4\left(T_{12} - f_V V_{12}\right)\left(T_{12}^* - f_V V_{12}\right) - 2T_{11}\left(T_{22} + f_V\left(V_{11} - V_{22}\right)\right) - 2f_V\left(T_{22} + f_V V_{11}\right)V_{22} + f_V^2 V_{22}^2 \right|}} \right|^2 \right)^{-\frac{1}{2}} \right) \quad (3)$$

In a first step a forward modeled Bragg surface scattering component is used to confine the volume scattering intensity f_v in a physical manner according to the approach in [3,5]. This constraint includes a variety of assumed dielectric levels (ε_s-levels), which are incorporated into the forward model. Hence, multiple solutions for different ε_s-levels are created and a unique solution will be found in the third step of the algorithm, as indicated in Fig. 2.

In the second step this physically constrained volume intensity component f_v is incorporated into the hybrid decomposition for separation of volume and ground scattering components. In contrast to [3] a generalized vegetation volume, included in [5], is proposed instead of the classical case of a random volume of dipoles:

$$T_V = f_v \begin{bmatrix} V_{11} & V_{12} & 0 \\ V_{12}^* & V_{22} & 0 \\ 0 & 0 & V_{33} \end{bmatrix} \quad (4)$$

$$= \frac{f_v}{1+A_p^2} \begin{bmatrix} \frac{1}{2}\left(A_p+1\right)^2 & \frac{1}{2}\left(A_p^2-1\right)\mathrm{sinc}(2\Delta\psi) & 0 \\ \frac{1}{2}\left(A_p^2-1\right)^2\mathrm{sinc}(2\Delta\psi) & \frac{1}{4}\left(A_p-1\right)^2\left(1+\mathrm{sinc}(4\Delta\psi)\right) & 0 \\ 0 & 0 & \frac{1}{4}\left(A_p-1\right)^2\left(1-\mathrm{sinc}(4\Delta\psi)\right) \end{bmatrix}$$

In Eq. 4 *Ap* denotes the particle anisotropy, which is linked to the shape of the vegetation constituents forming the volume. *Δψ* represents the distribution width of the orientation angles and stands for the degree of orientation of the particles within the vegetation volume. Fig. 3 characterizes the meaning of both volume parameters in a conceptual way [5].

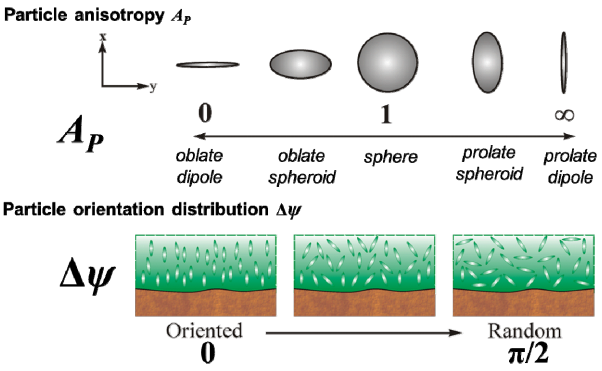

Figure 3: Conceptual description of vegetation volume parameters Ap (particle anisotropy) and Δψ (particle orientation distribution).

Within the first part of the hybrid decomposition a model-based removal of the volume scattering component (cf. Eq. 1) is conducted including the physical constrained volume intensity f_v to remove the vegetation contribution and to obtain the ground scattering components (surface, dihedral) [3,5].

Afterwards the second part of the hybrid decomposition involves an eigen-based separation of the surface from the dihedral scattering components. The corresponding intensities (f_d, f_s) and scattering mechanisms (α_d, α_s) of the ground components ($[T_G]=[T_S]+[T_D]$) can be calculated from the eigenvalues and eigenvectors of $[T_G]$ (cf. Eqs. 2-3). An orthogonality condition, proposed in [4], ensures the physically meaningful separation of surface from dihedral scattering as detailed in [3,5].

Hence, the surface/dihedral scattering contributions are extracted for a set of assumed ε_s-levels originating from the volume constraining.

Thus in the determination step, the corresponding ε_s-level for each pixel is found. Two alpha criteria enable the retrieval of the best matching ε_s-level for an optimum selection of the respective surface and dihedral scattering component after a physically constrained volume removal.

The first alpha criterion, called α_1-criterion, was already introduced in [3,5] and is refined for this approach by including an urban/forest mask before applying the criterion in order to exclude inappropriate scatterers from the evaluation. Hence a mean ε_s-level is defined for the entire scene. With the second alpha criterion, called α_{min}-criterion, a pixel-wise refinement of the mean ε_s-level is achieved, as depicted in Fig. 4.

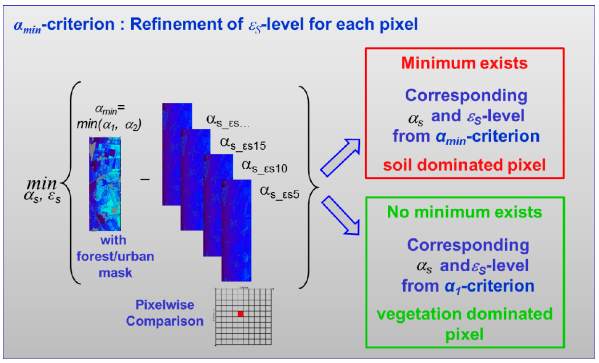

Figure 4: Schematic workflow of the α_{min}-criterion for a pixel-wise refinement of the ε_s-level determination.

Therefore α_{min} is calculated, which represents the minimum of the first and the second scattering alpha angle (α_1, α_2) of the eigen-decomposition of [T_{Data}]. This assures that for pixels, where the most dominant ground scattering in α_1 is dihedral and the surface scattering mechanism is located in α_2, the appropriate alpha angle, representing mostly surface scattering, is used for comparison with the α_s-solutions from the hybrid decomposition. Also for this criterion an urban/forest mask is applied to exclude inappropriate scatterers from the evaluation. Subsequently, the minimum between α_{min} and the multiple solutions for α_s is calculated pixel-wise to retrieve the corresponding ε_s-level. If no minimum can be found, the mean ε_s-level from the already applied α_1-criterion is used for the corresponding pixel. In the end the ε_s-level, the physically constrained f_v and the respective, decomposed surface scattering mechanism α_s are obtained for inversion of soil moisture

Hence, a low parameterized electro-magnetic surface scattering model (Bragg/ SPM) is applied to retrieve the closest match between modeled (β_m,) and decomposed surface scattering mechanism ($\beta=f(\alpha_s)$) for subsequent soil moisture (mv) inversion [3,5].

$$\text{Surface: } \text{mv} = \min\left\{\left|\beta - \beta_m\right|\right\} \quad \text{with} \quad \beta = -\tan(\alpha_s) \qquad (5)$$

β_m is the link to the volumetric soil moisture [3], because it is formed by the horizontal and vertical Bragg reflection coefficients (R_{HH}, R_{VV}) [5]. These coefficients depend only on the local incidence angle θ of the acquisition system and the dielectric constant of the soil ε_s. Finally, the dielectric constant ε_s is transformed into the volumetric soil moisture by a universal conversion polynomial of Topp *et al.* [6].

3. EXPERIMENTAL RESULTS

The refined, hybrid polarimetric decomposition and soil moisture inversion algorithm is applied on the data set of the TERENO campaigns, whereby the assumption of a random volume was applied within the generalized volume model (Ap=0, $\Delta\psi$=90°). The TERENO campaigns were conducted in May/June 2011 and in May 2012 by the Helmholtz Center for Environmental Research (UFZ), Water Earth System Science (WESS) Competence Cluster, Research Centre Jülich (FZJ), German Research Centre for Geoscience (GFZ) and the German Aerospace Center (DLR) within the TERENO observatories [7]. During these campaigns fully polarimetric L-band data were acquired by DLR's novel, high-resolution, airborne F-SAR system. The observatories feature medium topographic variations, a variety of soil and crop types (in different phenological stages) as well as different hydrological conditions (dry to medium moist). Simultaneously to the overflights, soil moisture and vegetation parameters were measured on selected test fields with a great variety of different crop and soil types to characterize the soil and the biomass layer.

Fig. 5 displays the results of the soil moisture inversion under vegetation for the TERENO 2012 campaign. The soil moisture is scaled for each data take individually, but always within the range of 0vol.% to 50vol.%. White areas represent non-physical results due to model mismatch in the inversion process, while forested as well as urban areas are masked gray.

The inversion rate is constantly on a very high level and does not drop below 98% for the two scenes, respectively. Compared to previous results in [3,5] the almost continuous and gapless inversion is also ensured for these data sets by application of the physically constrained hybrid decomposition and inversion for soil moisture under vegetation cover.

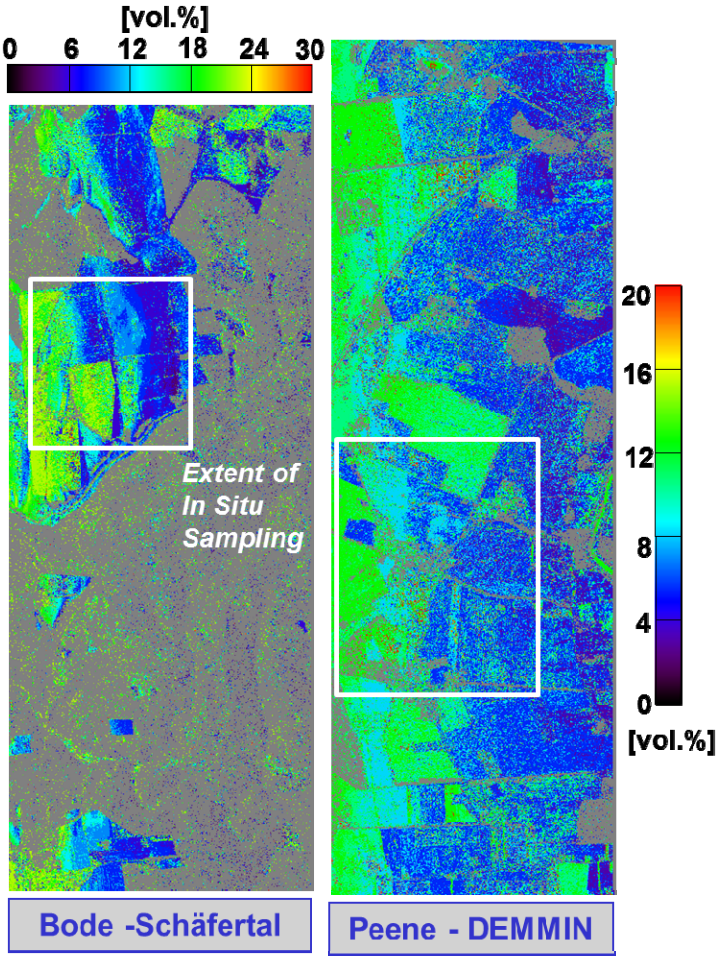

Figure 5: Results of soil moisture inversion under vegetation in vol.% for the TERENO 2012 campaign, conducted in the observatories of the Bode (Schäfertal) and the Peene (DEMMIN) catchment; Forested and urban areas are masked gray, while invalid regions are masked white. Additionally, white boxes indicate the areas, where in situ measurements were performed for validation.

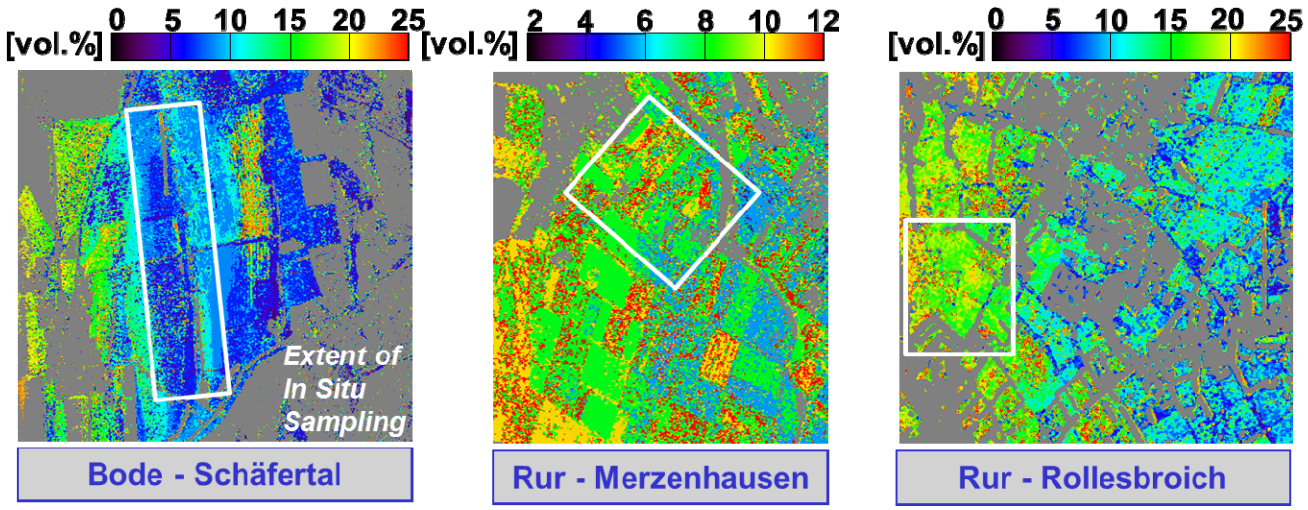

Figure 6: Results of soil moisture inversion under vegetation in vol.% for the TERENO 2011 campaign, conducted in the observatories of the Bode (Schäfertal) and the Rur catchment (Merzenhausen, Rollesbroich); Forested and urban areas are masked gray, while invalid regions are masked white. Additionally, white boxes indicate the areas, where in situ measurements were performed for validation.

In contrast to former results in [3,5] a dominant range trend in the soil moisture inversion results could be significantly reduced by the refinement of the algorithm, especially due to the pixel-wise determination of the ε_s-level with both α-criteria. In addition, also the level of detail and the contrast of the different moisture levels could be increased by the algorithm refinement, which is especially pronounced in the very dry case of the Merzenhausen test site within the Rur catchment (cf. Fig. 6 middle), including a variety of crop types on small parcels.

4. VALIDATION OF SOIL MOISTURE ESTIMATION

Ground measurements of soil moisture were taken with FDR probes (all test sites without Rollesbroich) and with a wireless soil moisture network (Rollesbroich test site) during the campaigns for a quantitative analysis of the inversion performance. A box of 13x13 pixels was drawn around each measurement location to realize 169 looks for comparison.

The resulting scatter plots of measured soil moistures on ground compared with estimated soil moistures from the developed approach are presented in Fig. 7-9 for the two TERENO campaigns (2011, 2012).

The measured soil moisture ranges approximately between 5vol.% and 20vol.% and states dry to medium moisture cases including all four different test sites (cf. Fig. 9). The SAR-based soil moistures stretch from 5vol.% to 25vol.% and indicate in general a slight overestimation. Especially the inversion results of 2011 for the Rollesbroich test site (blue color in Fig. 7) with the wireless soil moisture network exhibit the strongest trend and also pose the highest requirements to the decomposition and inversion algorithm. In this case a narrow *in situ* moisture range between 10vol.% and 15vol.% has to be met by the algorithm for a spatially varying grassland vegetation cover.

However, the validation with *in situ* measurements reveals a constantly high performance of the refined hybrid decomposition and inversion algorithm with a root mean square error of 6.1vol.% including all test sites (Bode, Peene, Rur) and all acquisition dates (2011, 2012).

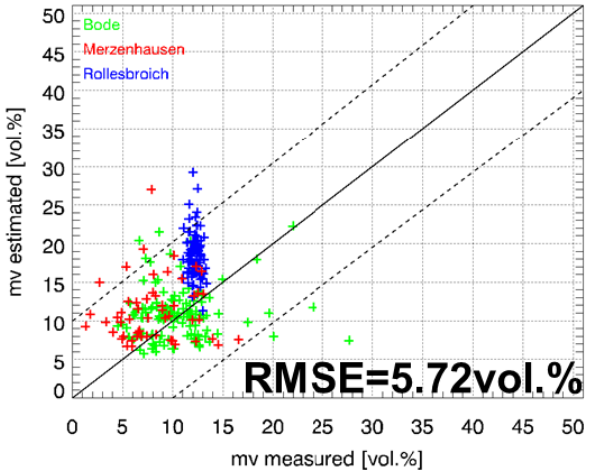

Figure 7: Scatter plots of measured soil moisture (mv) values from a wireless soil moisture network (Rollesbroich) and FDR (Bode, Merzenhausen) against estimated soil moisture values from the refined hybrid algorithm in vol.% for a variety of land use types (Bode: Winter wheat, summer wheat, grassland, winter triticale, Merzenhausen: Asparagus, grassland, sugar beet, potato, winter barley, winter wheat, Rollesbroich: Grassland).

This indicates the potential of the approach, while residual incidence effects can be found for the dry moisture case of the DEMMIN test site with an RMSE of 7.09vol.%.

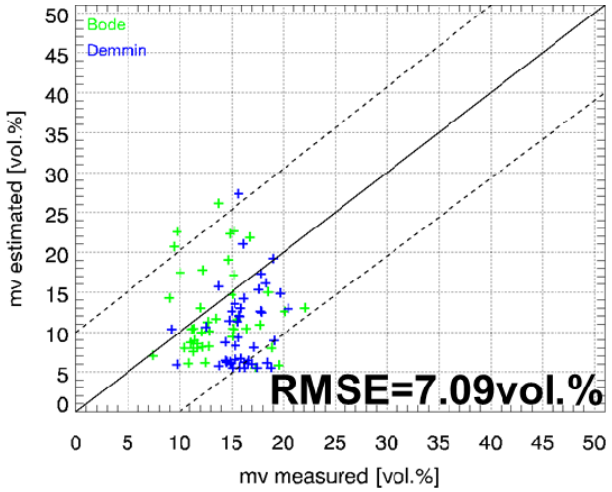

Figure 8: Scatter plots of measured soil moisture (mv) values from FDR probes against estimated soil moisture values from the refined hybrid algorithm in vol.% for a variety of land use types (Bode: Winter wheat, grassland, winter rape, DEMMIN: Sugar beet, summer corn).

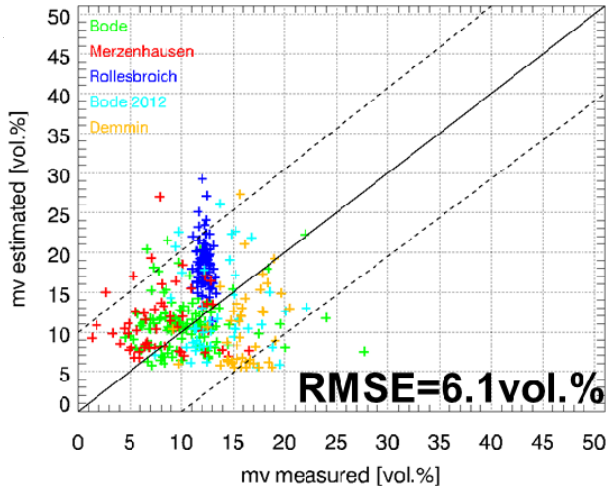

Figure 9: Combined scatter plot of both TERENO campaigns (2011 and 2012) and for all land use types.

5. SUMMARY AND CONCLUSIONS

Fully polarimetric L-band SAR data were acquired by DLR's novel, high-resolution F-SAR sensor together with *in situ* measurements of the TERENO campaigns within three of the four TERENO observatories (Bode, Peene, Rur) covering a variety of crop and soil types.

The refined, hybrid polarimetric decomposition and inversion algorithm for soil moisture inversion under vegetation cover was further developed and applied on the data set including a physically constrained volume intensity component.

The inversion rate remains in all investigated cases higher than 98% allowing an almost continuous and gapless inversion, which enables for the first time an analysis of spatial patterns within the areal moisture distribution.

Moreover, the refinement to retrieve the appropriate ε_s-level on a pixel-by-pixel basis establishing two α-criteria (e.g. Fig. 4) led to a distinct increase in level of detail for the spatial soil moisture distribution.

The inversion quality is assessed by a validation with FDR probe measurements and a comparison with a wireless soil moisture network (Rollesbroich test site). The RMSE-level ranges between 5.72vol.% (cf. Fig.7) and 7.09vol.% (cf. Fig.8) for the four test sites (five data takes) comprising a variety of agricultural vegetation types. Despite the promising overall RMSE of 6.1vol.%, residual range trends remained in the soil moisture inversion results and will be investigated by a multi-angular analysis. In addition, the vegetation volume model of Eq.4 will be applied in its general form for an upcoming generalized hybrid decomposition and inversion algorithm for soil moisture under vegetation cover.

ACKNOWLEDGMENTS

The authors would like to thank the TERENO members, Research Centre Jülich, Water Earth System Science (WESS) Competence Cluster, Helmholtz Centre for Environmental Research and German Center for Geosciences, for their great cooperation, including especially the provision of the field data from the observatories to validate the presented soil moisture retrieval algorithm. The *in situ* measurement systems were funded by the Terrestrial Environmental Observatories (TERENO) initiative of the German Helmholtz Association. A special thanks goes to the Federal Agency for Cartography and Geodesy of Germany for providing high-resolution digital elevation models.

REFERENCES

1. Bogena, H., Schulz, K., Vereecken, H. (2006) Towards a network of observatories in terrestrial environmental research. Advances in Geosciences 9, 1-6.
2. Bogena, H., Bens, O., Haschberger, P., Hajnsek, I., Dietrich, P., Priesack, E., Pütz, T., Munch, J.C., Papen, H., Schmid, H.P., Vereecken, H., Zacharias, S. (2010) Aktueller Stand zur Implementierung der TERENO Observatorien. Long Term Ecological

Research Annual Meeting, 22-24 March, National Park Eifel, Germany.
3. Jagdhuber, T., Hajnsek, I., Papathanassiou, K.P., Bronstert, A. (2012) Soil Moisture Retrieval Under Agricultural Vegetation Using Fully Polarimetric SAR. Proc. of IEEE International Geoscience and Remote Sensing Symposium, Munich, Germany, July 22-27, 1481-1484.
4. Cloude, S.R. (2010) *Polarisation: Applications in Remote Sensing*, Oxford, Oxford University, GB.
5. Jagdhuber, T. (2012) Soil Parameter Retrieval under Vegetation Cover Using SAR Polarimetry. PhD Thesis, http://nbn-resolving.de/urn:nbn:de:kobv:517-opus-60519, University of Potsdam, Potsdam, Germany.
6. Topp, G.C., Davis, J.L., Annan, A.P. (1980) Electromagnetic Determination of Soil Water Content: Measurements in Coaxial Transmission Lines. Water Resources Res., 16(3), 574-582.
7. Jagdhuber, T., Kohling, M., Hajnsek, I. (2011) TERENO F-SAR Airborne Campaign 2011 @ Rur, Bode and Ammer catchments. CT Environmental Sensing Meeting, DLR Oberpfaffenhofen, Germany, 29. November 2011.